miR-181b-5p mediates TGF-β1-induced epithelial-to-mesenchymal transition in non-small cell lung cancer stem-like cells derived from lung adenocarcinoma A549 cells

XUETAO LI[1], JING HAN[1], HAIZHEN ZHU[2], LINA PENG[1] and ZHENGTANG CHEN[1]

[1]Cancer Institute of PLA, Xinqiao Hospital, Third Military Medical University, Chongqing 400037;
[2]Department of Oncology, Guizhou Provincial People's Hospital, Guiyang, Guizhou 550002, P.R. China

Received March 25, 2017; Accepted May 9, 2017

DOI: 10.3892/ijo.2017.4007

Abstract. The ability of non-small cell lung cancer (NSCLC) cells to invade and metastasize is associated with epithelial-to-mesenchymal transition (EMT). The process of EMT is, at least in part, regulated by microRNAs. However, it is unknown whether microRNAs regulate EMT in cancer stem-like cells (CSLCs), or which microRNAs are involved. In the present study, we compared microRNA expression in A549 cells, TGF-β1-treated A549 cells, CSLCs characterized by the $CD133^+/CD326^+$ phenotype, and TGF-β1-treated CSLCs. We found that miR-181b-5p expression was upregulated by TGF-β1. Moreover, the overexpression of the miR-181b-5p in A549 cells and $CD133^+/CD326^+$ cells resulted in the down-regulation of the E-cadherin and increased invasion and metastasis *in vitro* and *in vivo*. Accordingly, the knockdown of miR-181b-5p partially restored E-cadherin expression. These results suggest that miR-181b-5p regulates TGF-β1-induced EMT by targeting E-cadherin not only in normal A549 cells but also in $CD133^+/CD326^+$ cells which have characteristics of CSLCs. Thus, miR-181b-5p represents a new therapeutic target in NSCLC.

Introduction

Non-small cell lung cancer (NSCLC) comprises 80-85% of lung cancer cases and is the leading cause of cancer deaths worldwide (1). Despite recent advances in understanding the molecular biology of lung cancer and the use of combined therapy including surgical resection, chemotherapy, radiation therapy and targeted therapy, the 5-year survival rate of NSCLC patients has not substantially changed. Only 15.9% of lung cancer patients survive ≥5 years, and ~50% of patients die of disease recurrence and metastasis (2).

The cancer stem cell (CSC) hypothesis suggests that a rare population of cancer cells with self-renewing capacity is responsible for tumor initiation, metastasis, relapse and therapeutic resistance (3,4). The existence of cancer stem-like cells (CSLCs) has been confirmed in hematopoietic malignancies and in solid tumors (5,6). CSLCs can be identified and isolated by spheroid formation in serum-free medium and by the expression of specific cell surface markers. Among the lung CSLC markers are $CD133^+$, $CD326^+$ (EpCAM), $CD44^+$, $ALDH1^+$ and Oct-4 (7-12). Some or all of these markers may be co-expressed to confer CSLCs properties. In our previous study, we demonstrated that a subpopulation of $CD133^+/CD326^+$ cells represents CSLC in the A549 cell line (13). CSLCs represent the ultimate target for cancer therapy.

Epithelial-to-mesenchymal transition (EMT) leads to the loss of epithelial cell adhesion and the acquisition of the mesenchymal phenotype (14,15). EMT plays a key role in the metastasis of NSCLC (16). Cancer cells treated with TGF-β1, an inducer of EMT, show decreased expression of E-cadherin and increased expression of vimentin, N-cadherin and matrix metalloproteinases (MMP), such as MMP-2, MMP-3 and MMP-9. Cells undergoing EMT also show increased motility and invasiveness. MicroRNAs are known to be critical regulators of EMT (17). The miR-200 family plays an essential role in suppressing the EMT through targeting ZEB in NSCLC and other cancers (18-20). miR-23a regulates TGF-β-induced EMT by targeting E-cadherin in lung cancer cells (21). The Snail and miR-34a-mediated regulation of ZNF281/ZBP99 promotes EMT (22). Accordingly, microRNAs can serve as novel therapeutic targets as well as diagnostic and prognostic markers in cancer (23).

To determine whether microRNAs also regulate EMT in CSLCs, we treated both A549 cells and $CD133^+/CD326^+$ cells with TGF-β1 and compared microRNA expression profiles. We demonstrated that both in A549 cells and $CD133^+/CD326^+$ cells, miR-181b-5p promotes tumor invasion and metastasis *in vitro* and *in vivo* by targeting the expression of E-cadherin.

Correspondence to: Dr Zhengtang Chen, Cancer Institute of PLA, Xinqiao Hospital, Third Military Medical University, 2 Xinqiao Street, Chongqing 400037, P.R. China
E-mail: czt05@163.com

Key words: miR-181b-5p, E-cadherin, epithelial-to-mesenchymal transition, cancer stem-like cells, non-small cell lung cancer

Materials and methods

Cell culture, TGF-β1 treatment and transfections. The human lung cancer cell line A549 was obtained from the American Type Culture Collection (ATCC) and was cultured in DMEM (Hyclone, USA) with 10% fetal bovine serum at 37˚C, 5% CO_2. The induced $CD133^+/CD326^+$ subpopulation cells were suspended in serum-free medium supplemented with 0.4% BSA (Sigma, USA), insulin (5 ng/ml, Sigma), bFGF (10 ng/ml, PeproTech, USA), EGF (20 ng/ml, PeproTech), and B27 (20 ng/ml, Invitrogen, USA) at a density of 10^3 cells/3 ml in ultralow attachment plates (Corning, USA).

To induce the EMT process, adherent A549 cells and $CD133^+/CD326^+$ spheroids were treated with 5 ng/ml TGF-β1 (Sigma) for 72 h. Adherent A549 cells and suspended $CD133^+/CD326^+$ cells were transfected with agomiR-181b-5p and antagomiR-181b-5p, which were purchased from RiboBio Co. Ltd. (China). Cells were plated in a 24-well plate at $1x10^5$ cells/plate. Agomirs or antagomirs of miR-181b-5p were appropriately diluted according to the manufacturer's protocol and added to the culture medium to transfect the cells. The concentration of agomiR-181b-5p and antagomiR-181b-5p were 50 nM and 100 nM, respectively. The expression of 181b-5p was determined 48 h after transfection.

Patients and peripheral blood samples. Peripheral blood samples were obtained from NSCLC patients prior to treatment at the Xinqiao Hospital of the Third Military Medical University between 2014 and 2015 and were stored at -80˚C. This project was approved by the ethics committee of the Xinqiao Hospital of the Third Military Medical University, and informed consent was obtained from all the patients.

Flow cytometry. Spheres were dissociated into single cells, washed and incubated with monoclonal antibodies specific for human CD133/1-PE and CD326-FITC (Miltenyi, Germany). The appropriate dilution and procedures were carried out according to the manufacturer's instructions. After incubation, the samples were washed with PBS and analyzed by FACSAria II (BD, USA). All $CD133^+/CD326^+$ cells were collected for subsequent experiments.

Quantitative real-time PCR. Total RNA was isolated using RNAiso Plus (Takara, Japan). Circulating microRNA in peripheral blood was isolated using the mirVana PARIS Kit (Ambion, USA). Reverse transcription reactions were performed using the PrimeScript™ RT reagent kit with gDNA Eraser (Takara) for mRNA and Bulge-Loop™ miRNA qRT-PCR Starter kit (RiboBio) for miRNA to make cDNA from total RNA in a MyCycler PCR system (Bio-Rad, USA). Subsequently, quantitative real-time PCR was performed using SYBR® Premix Ex Taq II (Takara). Primer pairs for miR-181b-5p, cel-miR-39 and U6 were purchased from RiboBio Co. Ltd. Primer pairs for GAPDH and genes associated with stemness and EMT were designed by Sangon Biotech Co. Ltd. (China). Each sample was performed in triplicate, and the reaction products were analyzed using the ABI 7500 Prism Sequence Detection system (Applied Biosystems, USA). Data analysis was based on the Ct method (ΔΔCt according to Applied Biosystems). All operations followed the manufacturer's protocol.

Immunofluorescence assay. Spheres were centrifuged (800 rpm, 5 min) on slides by cytospin and fixed with 4% paraformaldehyde and 0.1% Triton for 30 min, washed with PBS, blocked with BSA for 30 min at room temperature, and then incubated with primary antibodies at 4˚C overnight. Primary antibodies were rabbit monoclonal anti-CD133 (Abcam, UK) and goat polyclonal anti-CD326 (Santa Cruz, USA) at a dilution of 1:300. After washing, the spheroids were incubated with goat anti-rabbit IgG-FITC (Beyotime, China) and donkey anti-goat IgG-Cy3 (BioLegend, USA) fluorescent antibodies at a dilution of 1:400 for 30 min and protected from light. After DAPI staining for the nucleus, the spheres were observed under an Olympus confocal microscope.

MicroRNA expression profiling array and data analysis. Adherent A549 cells and $CD133^+/CD326^+$ cells were left untreated or were treated with TGF-β1 as described above. Cells were lysed using TRIzol (Life Technologies, USA) according to the manufacturer's instructions. First, *E. coli* poly(A) polymerase was used to generate polyadenylated tails at the 3'-end of all RNA molecules. Second, after annealing oligo-dT primers, cDNA was synthesized using the qScript Flex cDNA synthesis kit (Quanta Biosciences, USA) according to the manufacturer's instructions for gene-specific priming (a universal tag that would extend from the 3'-end of cDNA molecules was added during reverse transcription). With the addition of this universal tag, individual miRNAs were detected with miRNA-specific forward primers and a reverse universal primer mix. A SYBR Green-based quantitative real-time PCR method was used to quantify the relative expression of mature miRNAs. A total of 362 mature miRNAs were evaluated in the microRNA expression profiling array. miRNA expression was normalized by geometric mean-based global normalization using the Real-Time StatMiner (Integromics, Spain) analysis software. The array data were processed by bioinformatics analysis.

Western blot assay. For western blot analysis, 40 μg of total protein was resolved by SDS polyacrylamide gel (Boster, China) electrophoresis, and the proteins were then transferred onto polyvinylidene difluoride (PVDF) membranes (Millipore, USA). The membranes were incubated with the Blocking kit (Boster) for 1 h and then incubated overnight at 4˚C with antibodies from the EMT antibody sampler kit (1:1,000 dilution, Cell Signaling Technology, USA). The protein levels were normalized against GAPDH from the same sample (1:3,000 dilution, ZSGB-Bio, China). After three washes, the membranes were incubated for 1 h at 37˚C with species-specific horseradish peroxidase-conjugated secondary antibodies. The membranes were developed using an enhanced chemiluminescence (ECL) detection system followed by exposure to Hyperfilm ECL (Beyotime).

Transwell invasion assay. A Transwell invasion assay was performed using 24-well Transwell permeable supports with 8-μm pores (Corning). Cells ($2x10^5$) were suspended in 200 μl serum-free DMEM/F12 medium and seeded into the Transwell inserts coated with Matrigel (BD Biosciences, USA). The bottoms of the wells were filled with 500 μl complete medium containing 20% fetal bovine serum. All cells were incubated

Table I. Xenografts on nude mice (male, 6 weeks old).

Cell number	$1x10^6$	$1x10^5$	$1x10^4$	$1x10^3$
$CD133^+/CD326^+$ cells	-	5/5	5/5	0/5
A549 cells	5/5	0/5	0/5	-
Latency (day)	13	15	18	-

at 37˚C, 5% CO_2. After 24 h, the cells in the upper chamber were removed with cotton swabs and the filter membrane was fixed with 4% paraformaldehyde for 20 min. Subsequently, the remaining cells of the filter membrane in the lower chamber were stained with 0.1% crystal violet stain solution. From five randomly selected fields, the cells that had invaded through the membrane to the lower surface were counted under a light microscope.

In vivo xenograft experiments. Five-week-old male nude mice were purchased from the Chinese Academy of Medical Sciences (Beijing, China). To generate xenografts, serial dilutions ($1x10^6$, $1x10^5$, 1x10, and $1x10^3$) of A549 cells and $CD133^+/CD326^+$ cells were injected into the mice (n=5). Mice were monitored twice a week and sacrificed after 6 weeks.

Tumor metastasis assay. A549 cancer cells at $2x10^6$/100 μl were injected into the right armpit of the forelimb in all 10 mice. The mice were observed twice per week. When xenografts reached ~5x5 mm (after nearly 2 weeks), we randomly chose 5 mice and injected 1 nmol micrON™ agomiR-181b-5p every 3 days for 4 weeks. The other 5 mice injected with micrON agomiR-181b-5p negative control were the control group. After 6 weeks, all mice were sacrificed and metastases were observed. All mouse experiments were performed in accordance with local ethics guidelines.

Statistical analysis. The data are expressed as the means ± SD. Statistical analysis of data was assessed using the Student's t-test and one-way ANOVA with SPSS 18.0 software. Differences with $p<0.05$ were considered statistically significant.

Results

Establishment of non-small lung cancer stem-like cells from A549 cells. Only 0.1% of adherent A549 cells co-expressed CD133 and CD326 (Fig. 1A), which are markers of stem cells. To enrich the $CD133^+/CD326^+$ cells, A549 cells were resuspended in serum-free medium and grown as spheroids. We confirmed by flow cytometry that 44.2% cells in the spheroids co-expressed CD133 and CD326 (Fig. 1B). We collected $CD133^+/CD326^+$ cells for the subsequent experiments. Next, we studied the expression of stemness-associated genes, including CD133, CD326, OCT-4 and Nanog, using quantitative real-time PCR. We demonstrated that the expression of these genes was higher in $CD133^+/CD326^+$ cells compared to the adherent A549 cells ($p<0.05$, Fig. 1C). Immunofluorescence assay confirmed that most of the cells in spheroids co-expressed CD133/CD326 (Fig. 1D). We demonstrated that as few as $1x10^4$ $CD133^+/CD326^+$ cells generated tumor xenografts in nude mice, whereas $1x10^5$ unselected A549 cells failed to do so. All xenografts were confirmed as adenocarcinoma by histologic examination (Fig. 1E and Table I). According to these results and our previous study (13), we concluded that the $CD133^+/CD326^+$ cell subpopulation of A549 cells has the traits of CSLCs.

TGF-β1 promotes EMT both in CSLCs and non-CSLCs. TGF-β1 has been shown to induce EMT in cancer cells (24). We treated adherent A549 cells and $CD133^+/CD326^+$ cells with 5 ng/ml of TGF-β1 for 72 h. As expected, adherent A549 cells treated with TGF-β1 lost their epithelial morphology. Their shape had changed drastically, the junction between cells became loose and cells acquired a fibroblast-like appearance. In contrast, TGF-β1 treatment did not trigger significant morphological changes in the $CD133^+/CD326^+$ subpopulation (Fig. 2A). We used quantitative real-time PCR to assess the expression of E-cadherin, vimentin, Snail and Slug. We demonstrated that TGF-β1 treatment induced the upregulation of vimentin, Snail and Slug and the downregulation of E-cadherin in both adherent A549 cells and $CD133^+/CD326^+$ cells (Fig. 2B). This result indicates that although the distinctive morphological changes of cells undergoing EMT were not observed in $CD133^+/CD326^+$ cells, the expression of EMT-associated genes indicative of the epithelial to mesenchymal transition was observed in parental A549 cells and in $CD133^+/CD326^+$ cells. Cancer cells undergoing EMT are widely known to gain the ability to invade and metastasize. We used Transwell invasion assay to show that compared to control A549 cells, A549 cells treated with TGF-β1 have increased invasion potential through the Matrigel membrane. $CD133^+/CD326^+$ have an increased basal ability to invade compared to unselected A549 cells and TGF-β1 further increased their invasive capacity (Fig. 2C and D). Based on these results, we concluded that TGF-β1 promotes EMT both in CSLCs and non-CSLCs.

MicroRNA profile reveals differential miRNA expression in EMT and stem cell phenotype. To identify microRNAs involved in EMT and stem cell phenotype, we performed microRNA expression profiles in A549 cells, A549 cells treated with TGF-β1, $CD133^+/CD326^+$ cells and in $CD133^+/CD326^+$ cells treated with TGF-β1 using a quantitative real-time PCR miRNA expression profiling array. We identified common microRNAs between two groups (A549 vs A549/TGF-β1 and $CD133^+/CD326^+$ vs $CD133^+/CD326^+$/TGF-β1), their predicted target genes (n=1180) and their binding sites using the TargetScan and miRanda databases. We performed GO analysis and pathway analysis based on the Gene Ontology database and the KEGG database. Finally, according to the interactions between these genes and their corresponding microRNAs, we constructed a microRNA-gene network. The microRNAs in the network were evaluated by the degree, which is the number of target genes regulated by one microRNA. A high degree indicates that a large number of target genes is regulated by this particular miRNA. Similarly, the degree of the gene indicates the number of microRNAs targeting this gene. If a gene has a high degree, multiple microRNAs may target it. The key miRNA and gene in the network always have the highest degrees (Tables II and III). Several miRNAs in Table II have an established role in cancer;

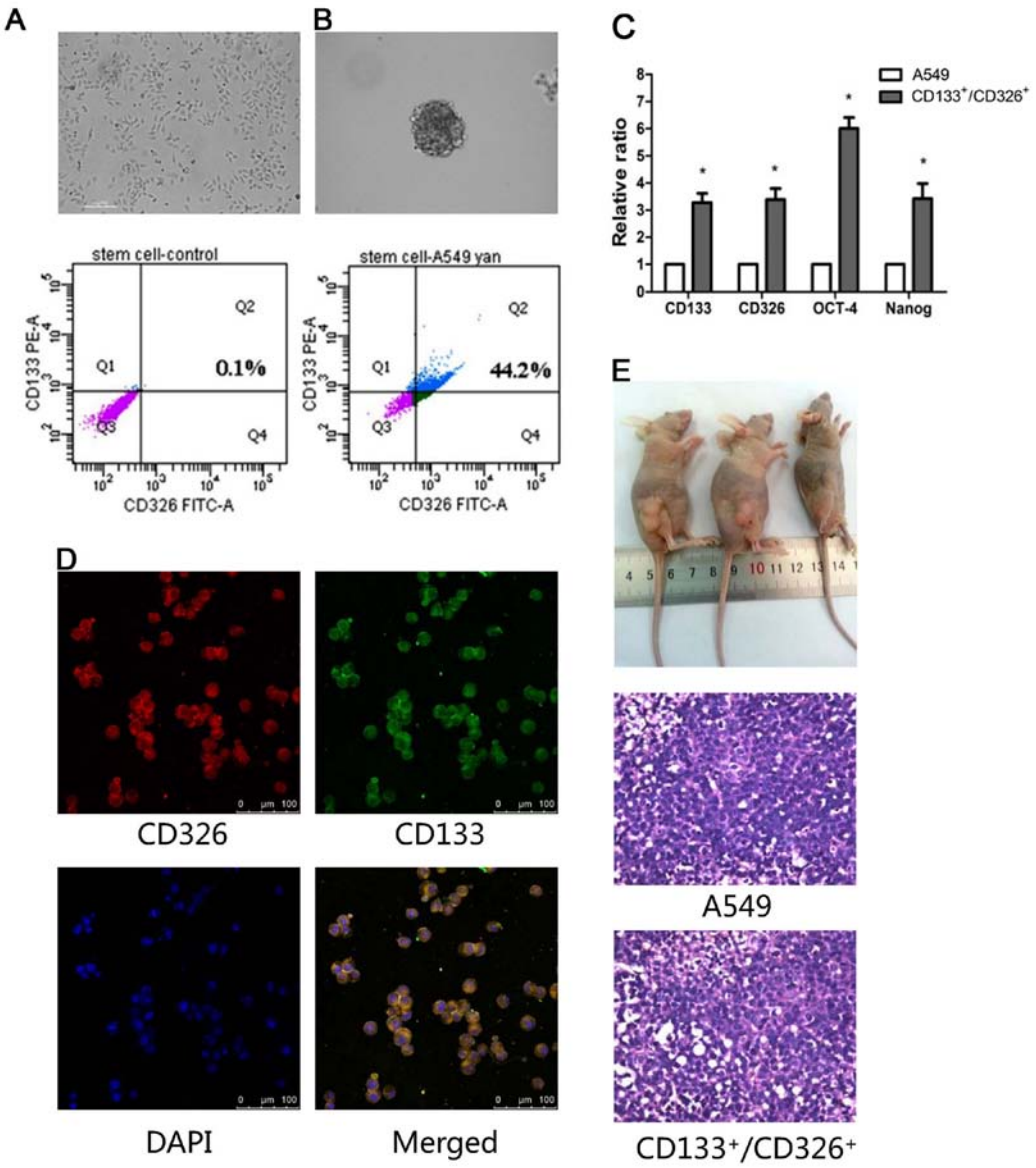

Figure 1. Identification of the CD133$^+$/CD326$^+$ subpopulation as CSLCs of A549. (A) The expression of CD133$^+$/CD326$^+$ in A549 cells. (B) The representative image of A549 spheroids in serum-free medium and the CD133$^+$/CD326$^+$ expression. (C) The expression of CD133, CD326, OCT-4 and Nanog in A549 cells and CD133$^+$/CD326$^+$ cells as measured by quantitative real-time PCR (*p<0.05). (D) Confocal microscopy of A549 spheroids in serum-free medium stained *in situ* with anti-CD133 antibody and anti-CD326 antibody; cell nuclei were counterstained with DAPI. (E) Xenografts in nude mice (left to right, 1x10^5, 1x10^4, 1x10^3 CD133$^+$/CD326$^+$ cells). All mice were sacrificed after 6 weeks and tumors were examined by H&E staining, x400.

Table II. The key microRNAs in the network (degree >20).

microRNA	A549/TGF-β1 vs A549	CD133$^+$/CD326$^+$/ TGF-β1 vs CD133$^+$/CD326$^+$	Degree
hsa-miR-497-5p	Down	Up	69
hsa-let-7e-5p	Up	Down	62
hsa-miR-671-5p	Up	Up	42
hsa-miR-302c-3p	Up	Up	37
hsa-miR-181b-5p	Up	Up	27
hsa-miR-302a-3p	Down	Up	25
hsa-miR-25-3p	Up	Up	23
hsa-miR-130b-3p	Up	Up	20

Table III. The target genes regulated mostly in the network (degree) >3.

Gene symbol	Description	Degree
PPARA	Peroxisome proliferator-activated receptor α	3
TGFA	Transforming growth factor, α	3
HDAC4	Histone deacetylase 4	3
ABL2	v-abl Abelson murine leukemia viral oncogene homolog 2	3
E2F3	E2F transcription factor 3	3
GABBR2	γ-aminobutyric acid (GABA) B receptor, 2	3
TPP1	Tripeptidyl peptidase I	3

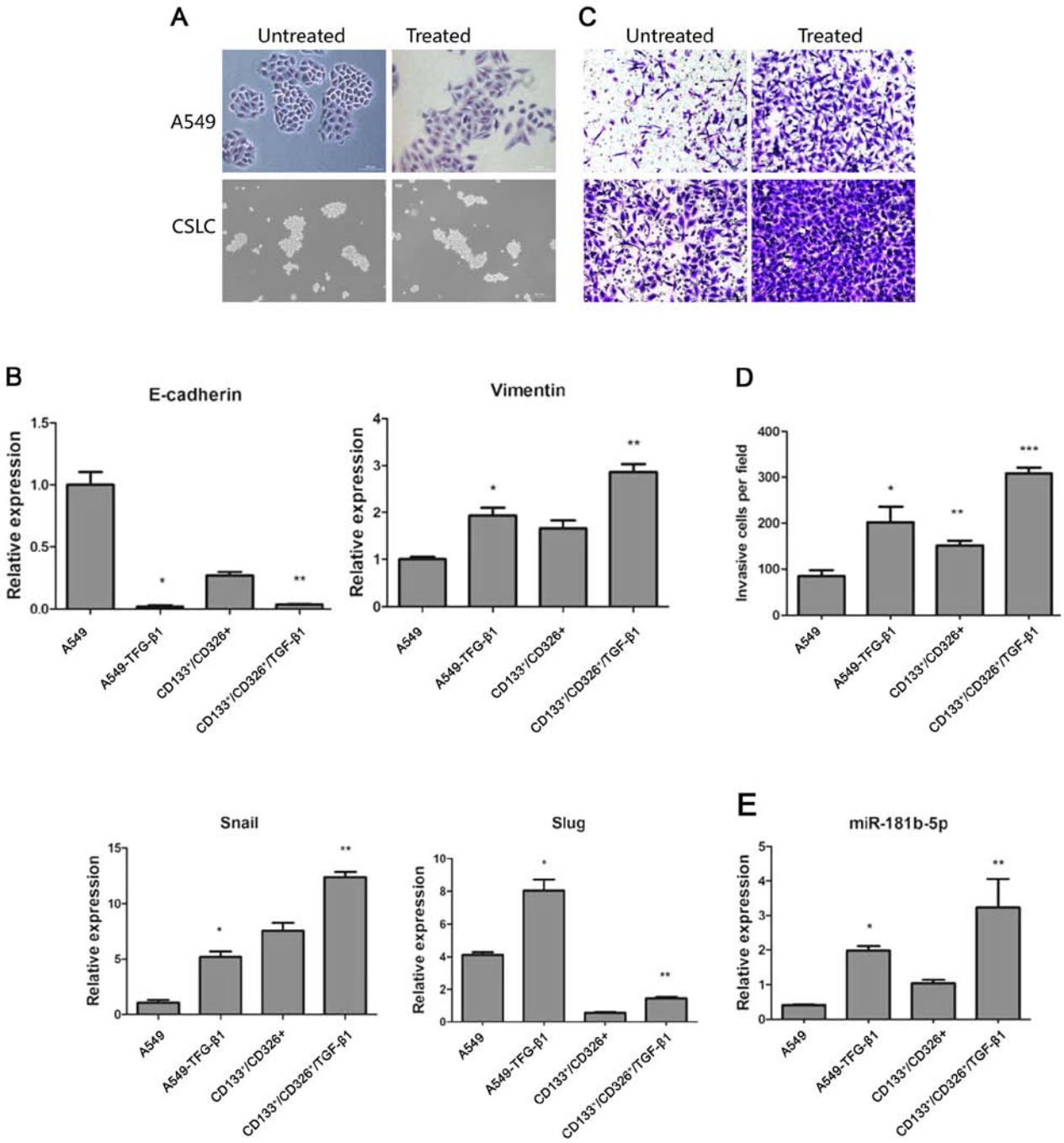

Figure 2. TGF-β1 promotes EMT in both CSLCs and non-CSLCs. (A) Microscope images of A549 cells and $CD133^+/CD326^+$ cells treated with TGF-β1. (B) Quantitative real-time PCR was used to measure the expression of E-cadherin, vimentin, Snail and Slug in untreated cells and in cells treated with TGF-β1 (*A549/TGF-β1 vs A549, $p<0.05$; $^{**}CD133^+/CD326^+/TGF-β1$ vs $CD133^+/CD326^+$, $p<0.05$). (C and D) Transwell invasion of untreated or TGF-β1-treated cells through the Matrigel membrane (*A549/TGF-β1 vs A549, $p<0.05$; $^{**}CD133^+/CD326^+$ vs A549, $p<0.05$; $^{***}CD133^+/CD326^+/TGF-β1$ vs A549, $p<0.05$). (E) Quantitative real-time PCR confirmed the expression levels of miR-181b-5p (*A549/TGF-β1 vs A549, $p<0.05$; $^{**}CD133^+/CD326^+/TGF-β1$ vs $CD133^+/CD326^+$, $p<0.05$).

however, the role of miR-181b-5p in EMT of CSLCs has not been described. We confirmed by quantitative real-time PCR that miR-181b-5p was significantly upregulated both in A549 and $CD133^+/CD326^+$ cells treated with TGF-β1 (Fig. 2E). We hypothesize that this may contribute to the invasion and metastasis of CSLCs and non-CSLCs.

miR-181b-5p is the key upregulator of EMT and targets E-cadherin in CSLCs and non-CSLCs. To modulate the expression of miR-181b-5p, we transfected agomiR-181b-5p into A549 cells and $CD133^+/CD326^+$ cells. In addition, we transfected antagomiR-181b-5p into A549 cells and $CD133^+/CD326^+$ cells that were treated with TGF-β1 for 72 h. We confirmed that the expression of miR-181b-5p in A549 cells and $CD133^+/CD326^+$ cells transfected with agomiR-181b-5p was increased 8.75- and 25.3-fold (Fig. 3A). Accordingly, the transfection of antagomiR-181b-5p into A549 cells and $CD133^+/CD326^+$ cells treated with TGF-β1

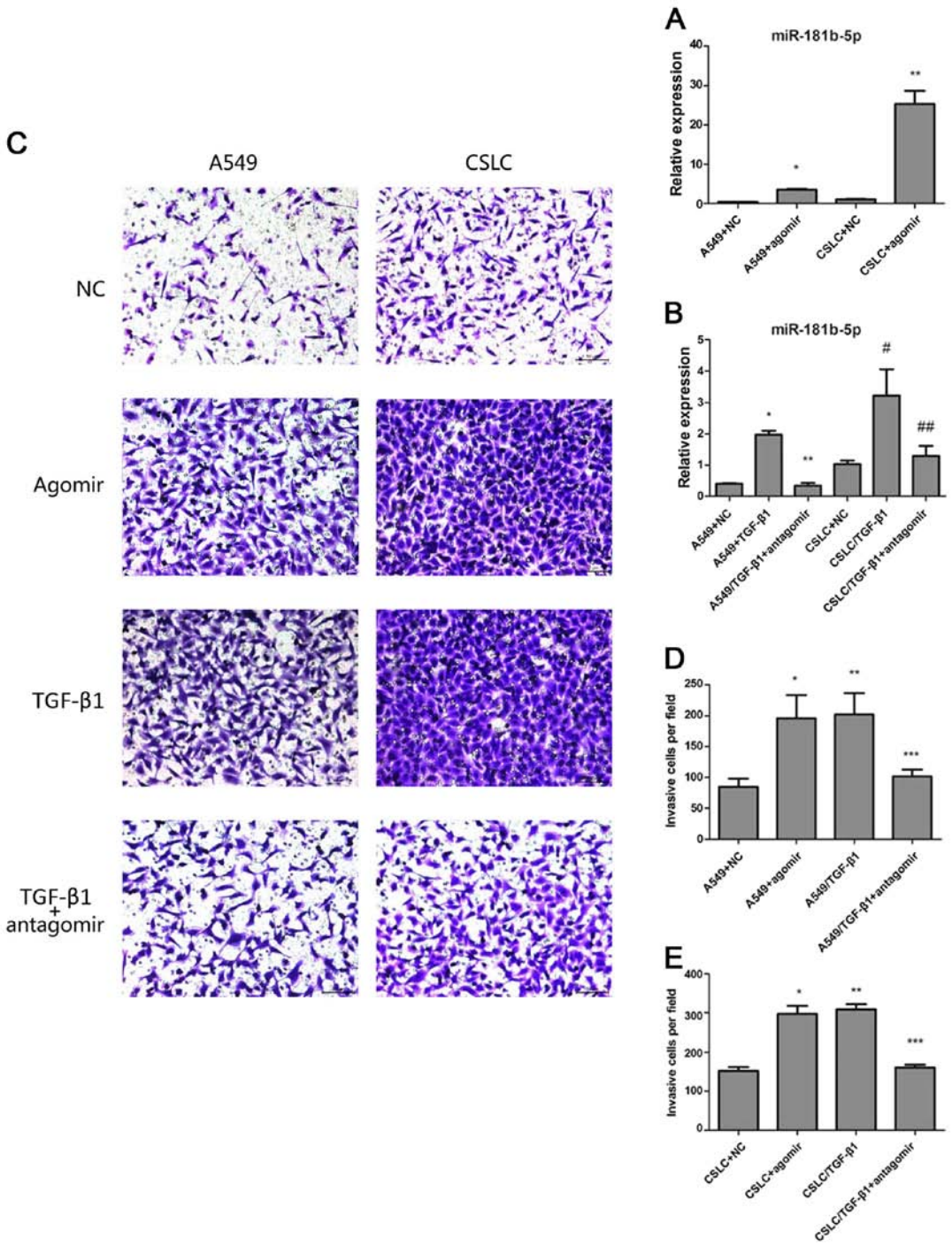

Figure 3. The effects of agomiR-181b-5p and antagomiR-181b-5p. (A) Quantitative real-time PCR measured the expression levels of miR-181b-5p in A549 cells and in CSLCs transfected with agomiR-181b-5p (* vs A549, $p<0.05$; ** vs CSLC $p<0.05$). (B) Quantitative real-time PCR was used to measure the expression levels of miR-181b-5p in A549/TGF-β1 and CSLC/TGF-β1 transfected with antagomiR-181b-5p (* vs A549/TGF-β1+antagomir $p<0.05$; $^{\#}$ vs CSLC/TGF-β1+antagomir, $p<0.05$; ** vs A549, $p=0.2529$; $^{\#\#}$ vs CSLC, $p=0.300$). (C) Detecting cell invasion by Transwell invasion assay. (D) The effect of agomiR-181b-5p and antagomiR-181b-5p on the invasion of A549 cells through the Matrigel membrane (* vs A549, $p<0.05$; ** vs A549+agomir, $p=0.6443$; *** vs A549, $p<0.05$). (E) The effect of agomiR-181b-5p and antagomiR-181b-5p on the invasion CSLCs through the Matrigel membrane (* vs CSLC, $p<0.05$; ** vs CSLC+agomir, $p=0.0818$; *** vs CSLC, $p<0.05$).

significantly reduced the expression of miR-181b-5p (Fig. 3B). This result confirmed that agomiR-181b-5p was the agonist of miR-181b-5p and that antagomiR-181b-5p was the antagonist of miR-181b-5p.

Next, we sought to determine whether miR-181b-5p regulates EMT *in vitro* and *in vivo*. Transwell invasion assay confirmed that agomiR-181b-5p, similar to TGF-β1 treatment, significantly enhanced the invasion of both A549 cells and $CD133^{+}/CD326^{+}$ cells. In contrast, antagomiR-181b-5p reduced the TGF-β1-mediated invasion in A549 cells and $CD133^{+}/CD326^{+}$ cells but did not completely eliminate the effect of TGF-β1 (Fig. 3C-E). We treated adherent A549 cells with 50 nM of agomiR-181b-5p for 7 days and observed that a part of adherent A549 cells lost their epithelial morphology

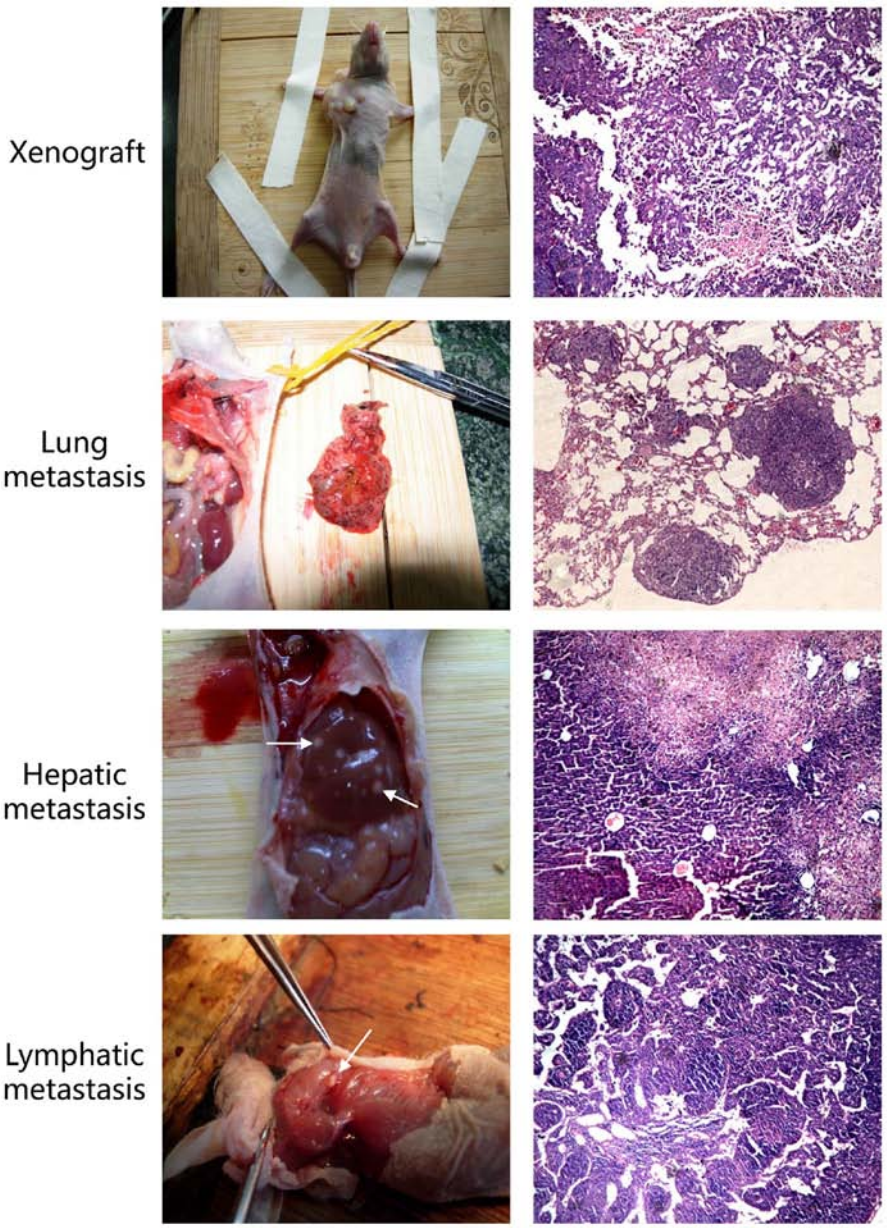

Figure 4. Xenografts and metastasis. Histologic examination (H&E, x100) revealed many micrometastases in the lungs and liver. We also observed necrosis on the liver surface in some nude mice and enlarged lymph nodes.

Table IV. Metastasis on nude mice.

Metastasis sites	A549+NC	A549+agomir
Lung	1	3
Liver	1	4
Lymph node	2	4

and acquired a fibroblast-like appearance (Fig. 5D). These results indicated that the expression of miR-181b-5p correlates with the ability of cells to invade in both CSLCs and non-CSLCs and that miR-181b-5p contributes to TGF-β1-induced EMT. Based on the *in vitro* studies, we hypothesized that the overexpression of miR-181b-5p may promote metastasis *in vivo*. To confirm this critical question, we performed a tumor metastasis assay and observed that the group of mice injected with agomiR-181b-5p had more metastasis than the negative control (Fig. 4 and Table IV). Thus, our findings suggest that miR-181b-5p promotes invasion and metastasis both in CSLCs and non-CSLCs *in vitro* and *in vivo*.

To identify the target gene of miR-181b-5p, we evaluated the expression of EMT markers (such as E-cadherin, vimentin, Snail and Slug) after the treatment of miR-181b-5p agomir and antagomir in untreated or TGF-β1 treated A549 cells and $CD133^+/CD326^+$ cells. After treatment with agomiR-181b-5p, decreased E-cadherin expression was observed only in A549 cells and $CD133^+/CD326^+$ cells (Fig. 5A). In contrast, antagomiR-181b-5p increased the expression of E-cadherin expression in TGF-β1-treated A549 cells and $CD133^+/CD326^+$ cells (Fig. 5B). Western blot analysis was used to detect the protein levels of E-cadherin and to confirm our results

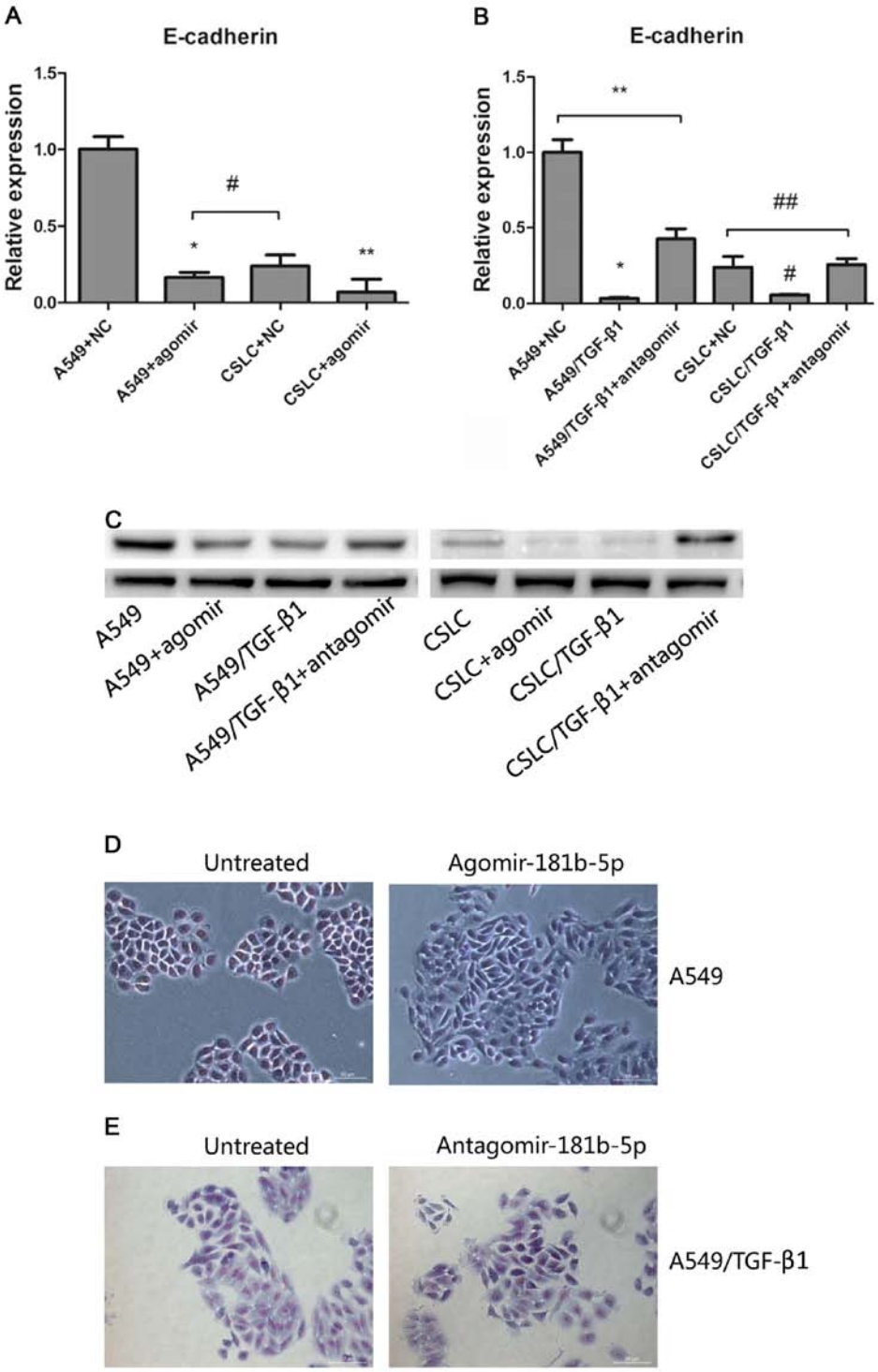

Figure 5. Regulation of E-cadherin expression by miR-181b-5p. (A) Quantitative real-time PCR of E-cadherin expression in A549 cells and CSLCs transfected with agomiR-181b-5p (* vs A549, p<0.05; ** vs CSLC, p<0.05; $^{\#}$p=0.1767). (B) Quantitative real-time PCR of E-cadherin expression in A549 cells and CSLCs transfected with antagomiR-181b-5p (* vs A549/TGF-β1+antagomir p<0.05; $^{\#}$ vs CSLC/TGF-β1+antagomir p<0.05; **p<0.05; $^{\#\#}$p=0.7267). (C) The expression of the protein levels of E-cadherin in A549 cells and CSLCs transfected with agomiR-181b-5p or antagomiR-181b-5p. (D) Microscope images of A549 cells and A549 cells treated with agomiR-181b-5p. (E) Microscope images of A549/TGF-β1 cells and A549/TGF-β1 cells treated with antagomiR-181b-5p.

(Fig. 5C). These findings suggested that miR-181b-5p promotes EMT at least in part by targeting E-cadherin in CSLCs and non-CSLCs.

Circulating miR-181b-5p is a potential clinical diagnostic marker. Finally, we compared the expression of miR-181b-5p in peripheral blood of 15 healthy people and 20 patients with NSCLC (patient characteristics are indicated in Table V). We found that the levels of miR-181b-5p in peripheral blood were increased in NSCLC patients (Fig. 6A) compared to healthy individuals (p<0.05). miR-181b-5p was upregulated in stage II/III/IV NSCLC patients (Fig. 6B, p<0.05). According to this result, miR-181b-5p may be a potential therapeutic target and a prognostic marker in NSCLC patients.

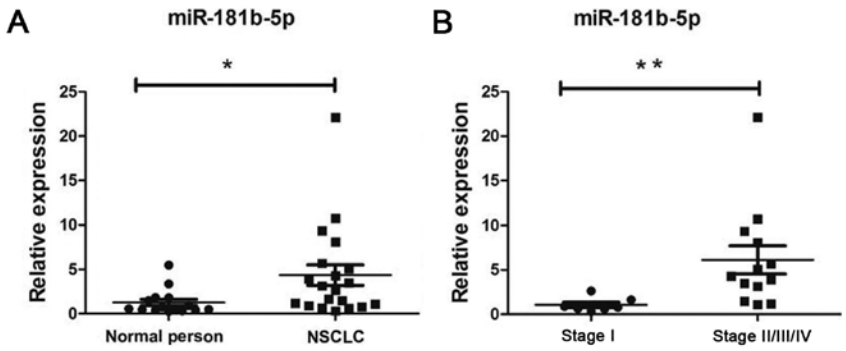

Figure 6. Quantitative real-time PCR detection of the expression of miR-181b-5p in peripheral blood between normal person and patients with NSCLC. (A) Quantitative real-time PCR measured the expression levels of miR-181b-5p in peripheral blood between normal person and patients with NSCLC ($^{*}p<0.05$). (B) Quantitative real-time PCR measured the expression levels of miR-181b-5p in different stages of NSCLC in peripheral blood. miR-181b-5p was significantly upregulated in stage II/III/IV NSCLC ($^{**}p<0.05$).

Table V. Clinical data statistics of NSCLC patients.

Items	No. of patients (n=20)
Age (year)	
≤60	8
>60	12
Sex	
Male	14
Female	6
Differerntiation	
Well	3
Moderate	4
Poor	13
Histology	
Non-adenocarcinoma	9
Adenocarcinoma	11
Lymph node metastasis	
Yes	11
No	9
TNM stage	
I	7
II	8
III	4
IV	1

Discussion

EMT is characterized by the loss of cellular polarity and adhesion and by enhanced invasive and migratory properties. Tumor cells treated with TGF-β1 have been shown to display decreased expression of E-cadherin and cytokeratins while overexpressing vimentin and N-cadherin, which is a hallmark of EMT (21,25). Studies of circulating tumor cells (CTCs) have shown that a subpopulation of CTCs shows characteristics of EMT, such as the overexpression of Twist, Snail, Slug, vimentin and FOXC1, and suggested that EMT induced by TGF-β1 is linked to the metastatic spread of cancer cells (26,27). Tumor cells that acquire a mesenchymal phenotype are released into peripheral blood; however, not all of these can form metastases. The cancer stem cell hypothesis suggests that the rare population of cancer cells that establishes metastases has characteristics of CSCs. However, there is heterogeneity among CSCs. Brabletz *et al* (28) proposed the concept of migratory CSCs. Compared to stationary CSCs, migratory CSCs gain migratory and metastatic properties by undergoing EMT in the primary tumor. In squamous cell carcinoma (SCC), Biddle *et al* (29) found that $CD44^{high}ESA^{high}$ cells retained epithelial characteristics (non-EMT CSCs) and that $CD44^{high}ESA^{low}$ cells were migratory and had mesenchymal traits characteristic of EMT CSCs. In this study, we investigated whether TGF-β1 can induce EMT in both CSCs and non-CSCs during the initial stage of tumor metastasis in NSCLC.

For this purpose, we sorted a $CD133^{+}/CD326^{+}$ cell subpopulation from A549 cells cultured in serum-free medium. These cells overexpressed stemness-associated genes, show increased tumorigenicity, and could be regarded as CSLCs. After treatment with TGF-β1, the expression of vimentin, Snail and Slug was upregulated both in CSLCs and in unsorted A549 cells. In contrast, the expression of E-cadherin was decreased by TGF-β1. Consistent with apparent EMT, CSLCs treated with TGF-β1 had the strongest capacity to invade in Transwell invasion assay. Thus, we concluded that both CSLCs and non-CSLCs can undergo EMT. The goal of this study was to assess the contribution of microRNAs in CSLCs undergoing EMT.

To establish the effect of TGF-β1 treatment on the expression of microRNAs in non-stem cells and CSLCs, we compared the expression of microRNAs between two pairs of treatment groups: A549 vs A549/TGF-β1 and $CD133^{+}/CD326^{+}$ vs $CD133^{+}/CD326^{+}$/TGF-β1. Four microRNA expression profiles, A549, A549/TGF-β1, $CD133^{+}/CD326^{+}$ and $CD133^{+}/CD326^{+}$/TGF-β1, were analyzed using bioinformatics approaches, including GO analysis, pathway analysis and graph theory (30-33) (Table II). Several miRNAs have an established role in EMT; however, the function of miR-181b-5p in promoting EMT in CSCs has not been reported. We therefore focused on the role of miR-181b-5p in EMT.

Previous studies showed that miR-181b functions as a tumor suppressor or a tumor promoter in different human malignancies (34-36). However, miR-181b-5p was rarely reported in lung

cancer. Liu *et al* (37) reported that miR-181b is downregulated in NSCLC tissues compared with the normal adjacent tissues. In contrast, Cinegaglia *et al* (38) found that miR-181b was overexpressed in lung adenocarcinoma compared to normal lung tissue. Similar results have been recently reported. Tian *et al* (39) characterized the expression profiles of miRNAs in sera and in tissues collected from NSCLC patients and found that miR-181b-5p was upregulated in serum and tissue of SCC patients. In our study, we modulated the expression of miR-181b-5p in A549 cells and $CD133^+/CD326^+$ cells and found that miR-181b-5p enhanced invasion and metastasis *in vitro* and *in vivo*. E-cadherin expression was negatively correlated with miR-181b-5p expression, suggesting that E-cadherin may be a target gene of miR-181b-5p. However, we observed that not all of normal A549 cells treated with agomiR-181b-5p lost their epithelial morphology and A549/TGF-β1 cells treated with antagomiR-181b-5p did not lose their mesenchymal morphology observably (Fig. 5D and E), implying a lack of direct correlation between E-cadherin expression and morphology. Additionally, CDH1 was not identified as a potential target gene of miR-181b-5p, suggesting that miR-181b-5p does not directly bind to E-cadherin mRNA. Transfection of TGF-β1-treated A549 cells or CSLCs with antagomiR-181b-5p did not reduce their invasive capacity to the levels of untreated cells (Fig. 3C-E), demonstrating that miR-181b-5p is one of several regulators involved in TGF-β1-dependent EMT.

Finally, we compared the levels of miR-181b-5p in peripheral blood of healthy humans and in patients with NSCLC. We found that the levels of miR-181b-5p were increased in peripheral blood of NSCLC patients and specifically in patients with stage II/III/IV disease. These data and the results discussed above suggest that miR-181b-5p may be a diagnostic biomarker of NSCLCs.

In conclusion, this study provides evidence that miR-181b-5p mediates TGF-β1-induced EMT by suppressing E-cadherin expression both in normal A549 cells and $CD133^+/CD326^+$ cells which have characteristics of CSLCs. miR-181b-5p may be a diagnostic marker and a new therapeutic target in NSCLC. Further studies are required to reveal the mechanism of miR-181b-5p suppression of the E-cadherin expression and to analyze the association between miR-181b-5p and NSCLC.

Acknowledgements

This study was supported by grants in aid (CSTC, 2011AB5032) from Chongqing Science and Technology Commission, China. We are grateful to Dr Sheng Lin from the Oncology Department, The Affiliated Hospital of Southwest Medical University for helpful discussion and Dr Xinwei Diao from the Pathology Department of Xinqiao Hospital for pathologic technical support.

References

1. Gupta G, Singh R, Kotasthane DS and Kotasthane VD: Myelodysplastic syndromes/neoplasms: Recent classification system based on World Health Organization Classification of Tumors - International Agency for Research on Cancer for Hematopoietic and Lymphoid Tissues. J Blood Med 1: 171-182, 2010.
2. Jemal A, Siegel R, Xu J and Ward E: Cancer statistics, 2010. CA Cancer J Clin 60: 277-300, 2010.
3. Ghotra VP, Puigvert JC and Danen EH: The cancer stem cell microenvironment and anti-cancer therapy. Int J Radiat Biol 85: 955-962, 2009.
4. Kreso A and Dick JE: Evolution of the cancer stem cell model. Cell Stem Cell 14: 275-291, 2014.
5. Florian S, Sonneck K, Hauswirth AW, Krauth MT, Schernthaner GH, Sperr WR and Valent P: Detection of molecular targets on the surface of $CD34^+/CD38^-$ stem cells in various myeloid malignancies. Leuk Lymphoma 47: 207-222, 2006.
6. Al-Hajj M, Wicha MS, Benito-Hernandez A, Morrison SJ and Clarke MF: Prospective identification of tumorigenic breast cancer cells. Proc Natl Acad Sci USA 100: 3983-3988, 2003.
7. Sarvi S, Mackinnon AC, Avlonitis N, Bradley M, Rintoul RC, Rassl DM, Wang W, Forbes SJ, Gregory CD and Sethi T: $CD133^+$ cancer stem-like cells in small cell lung cancer are highly tumorigenic and chemoresistant but sensitive to a novel neuropeptide antagonist. Cancer Res 74: 1554-1565, 2014.
8. Pak MG, Shin DH, Lee CH and Lee MK: Significance of EpCAM and TROP2 expression in non-small cell lung cancer. World J Surg Oncol 10: 53, 2012.
9. Zakaria N, Yusoff NM, Zakaria Z, Lim MN, Baharuddin PJ, Fakiruddin KS and Yahaya B: Human non-small cell lung cancer expresses putative cancer stem cell markers and exhibits the transcriptomic profile of multipotent cells. BMC Cancer 15: 84, 2015.
10. Leung EL, Fiscus RR, Tung JW, Tin VP, Cheng LC, Sihoe AD, Fink LM, Ma Y and Wong MP: Non-small cell lung cancer cells expressing CD44 are enriched for stem cell-like properties. PLoS One 5: e14062, 2010.
11. Jiang F, Qiu Q, Khanna A, Todd NW, Deepak J, Xing L, Wang H, Liu Z, Su Y, Stass SA, *et al*: Aldehyde dehydrogenase 1 is a tumor stem cell-associated marker in lung cancer. Mol Cancer Res 7: 330-338, 2009.
12. Chen YC, Hsu HS, Chen YW, Tsai TH, How CK, Wang CY, Hung SC, Chang YL, Tsai ML, Lee YY, *et al*: Oct-4 expression maintained cancer stem-like properties in lung cancer-derived CD133-positive cells. PLoS One 3: e2637, 2008.
13. Lin S, Sun JG, Wu JB, Long HX, Zhu CH, Xiang T, Ma H, Zhao ZQ, Yao Q, Zhang AM, *et al*: Aberrant microRNAs expression in $CD133^+/CD326^+$ human lung adenocarcinoma initiating cells from A549. Mol Cell 33: 277-283, 2012.
14. Brabletz T: EMT and MET in metastasis: Where are the cancer stem cells? Cancer Cell 22: 699-701, 2012.
15. Thiery JP and Lim CT: Tumor dissemination: An EMT affair. Cancer Cell 23: 272-273, 2013.
16. Tu Z, Xie S, Xiong M, Liu Y, Yang X, Tembo KM, Huang J, Hu W, Huang X, Pan S, *et al*: CXCR4 is involved in CD133-induced EMT in non-small cell lung cancer. Int J Oncol 50: 505-514, 2017.
17. Abba ML, Patil N, Leupold JH and Allgayer H: MicroRNA regulation of epithelial to mesenchymal transition. J Clin Med 5: 5, 2016.
18. Gibbons DL, Lin W, Creighton C, Zhang S, Lozano G and Kurie J: Use of a murine model of NSCLC to evaluate the role of the microRNA-200 family in regulating EMT and metastasis. J Clin Oncol 27: 11006, 2009.
19. Park SM, Gaur AB, Lengyel E and Peter ME: The miR-200 family determines the epithelial phenotype of cancer cells by targeting the E-cadherin repressors ZEB1 and ZEB2. Genes Dev 22: 894-907, 2008.
20. Nishijima N, Seike M, Soeno C, Chiba M, Miyanaga A, Noro R, Sugano T, Matsumoto M, Kubota K and Gemma A: miR-200/ZEB axis regulates sensitivity to nintedanib in non-small cell lung cancer cells. Int J Oncol 48: 937-944, 2016.
21. Cao M, Seike M, Soeno C, Mizutani H, Kitamura K, Minegishi Y, Noro R, Yoshimura A, Cai L and Gemma A: miR-23a regulates TGF-β-induced epithelial-mesenchymal transition by targeting E-cadherin in lung cancer cells. Int J Oncol 41: 869-875, 2012.
22. Hahn S, Jackstadt R, Siemens H, Hünten S and Hermeking H: SNAIL and miR-34a feed-forward regulation of ZNF281/ZBP99 promotes epithelial-mesenchymal transition. EMBO J 32: 3079-3095, 2013.
23. Díaz-López A, Moreno-Bueno G and Cano A: Role of microRNA in epithelial to mesenchymal transition and metastasis and clinical perspectives. Cancer Manag Res 6: 205-216, 2014.
24. Derynck R, Muthusamy BP and Saeteurn KY: Signaling pathway cooperation in TGF-β-induced epithelial-mesenchymal transition. Curr Opin Cell Biol 31: 56-66, 2014.
25. Ma M, He M, Jiang Q, Yan Y, Guan S, Zhang J, Yu Z, Chen Q, Sun M, Yao W, *et al*: miR-487a promotes TGF-β1-induced EMT, the migration and invasion of breast cancer cells by directly targeting MAGI2. Int J Biol Sci 12: 397-408, 2016.

26. Yu M, Bardia A, Wittner BS, Stott SL, Smas ME, Ting DT, Isakoff SJ, Ciciliano JC, Wells MN, Shah AM, *et al*: Circulating breast tumor cells exhibit dynamic changes in epithelial and mesenchymal composition. Science 339: 580-584, 2013.
27. Kallergi G, Papadaki MA, Politaki E, Mavroudis D, Georgoulias V and Agelaki S: Epithelial to mesenchymal transition markers expressed in circulating tumour cells of early and metastatic breast cancer patients. Breast Cancer Res 13: R59, 2011.
28. Brabletz T, Jung A, Spaderna S, Hlubek F and Kirchner T: Opinion: Migrating cancer stem cells - an integrated concept of malignant tumour progression. Nat Rev Cancer 5: 744-749, 2005.
29. Biddle A, Liang X, Gammon L, Fazil B, Harper LJ, Emich H, Costea DE and Mackenzie IC: Cancer stem cells in squamous cell carcinoma switch between two distinct phenotypes that are preferentially migratory or proliferative. Cancer Res 71: 5317-5326, 2011.
30. Gene Ontology C; Gene Ontology Consortium: The Gene Ontology (GO) project in 2006. Nucleic Acids Res 34: D322-D326, 2006.
31. Draghici S, Khatri P, Tarca AL, Amin K, Done A, Voichita C, Georgescu C and Romero R: A systems biology approach for pathway level analysis. Genome Res 17: 1537-1545, 2007.
32. Guo CJ, Pan Q, Li DG, Sun H and Liu BW: miR-15b and miR-16 are implicated in activation of the rat hepatic stellate cell: An essential role for apoptosis. J Hepatol 50: 766-778, 2009.
33. Joung JG, Hwang KB, Nam JW, Kim SJ and Zhang BT: Discovery of microRNA-mRNA modules via population-based probabilistic learning. Bioinformatics 23: 1141-1147, 2007.
34. Zhi F, Shao N, Wang R, Deng D, Xue L, Wang Q, Zhang Y, Shi Y, Xia X, Wang S, *et al*: Identification of 9 serum microRNAs as potential noninvasive biomarkers of human astrocytoma. Neuro Oncol 17: 383-391, 2015.
35. Zheng Y, Lv X, Wang X, Wang B, Shao X, Huang Y, Shi L, Chen Z, Huang J and Huang P: miR-181b promotes chemoresistance in breast cancer by regulating Bim expression. Oncol Rep 35: 683-690, 2016.
36. Wang J, Sai K, Chen FR and Chen ZP: miR-181b modulates glioma cell sensitivity to temozolomide by targeting MEK1. Cancer Chemother Pharmacol 72: 147-158, 2013.
37. Liu Y, Hu X, Xia D and Zhang S: MicroRNA-181b is downregulated in non-small cell lung cancer and inhibits cell motility by directly targeting HMGB1. Oncol Lett 12: 4181-4186, 2016.
38. Cinegaglia NC, Andrade SC, Tokar T, Pinheiro M, Severino FE, Oliveira RA, Hasimoto EN, Cataneo DC, Cataneo AJ, Defaveri J, *et al*: Integrative transcriptome analysis identifies deregulated microRNA-transcription factor networks in lung adenocarcinoma. Oncotarget 7: 28920-28934, 2016.
39. Tian F, Shen Y, Chen Z, Li R, Lu J and Ge Q: Aberrant miR-181b-5p and miR-486-5p expression in serum and tissue of non-small cell lung cancer. Gene 591: 338-343, 2016.